Paper Published as:

Tancredi, U.; Grassi, M.; Corraro, F.; Vitale, A. & Filippone, E. (2012), 'A linear time-varying approach for robustness analyses of a re-entry flight technology demonstrator', Proceedings of the Institution of Mechanical Engineers Part G-journal of Aerospace Engineering ***226****(G4), 467--480.*

Doi 10.1177/0954410011409305

A linear time varying approach for robustness analyses of a re-entry flight technology demonstrator

Urbano Tancredi [1]
University of Naples Parthenope, Napoli, 80143, Italy

Michele Grassi [2]
University of Naples Federico II, Napoli, 80125, Italy

Federico Corraro[3], Antonio Vitale[4] and Edoardo Filippone[5]
Italian Aerospace Research Centre, Capua, (CE), 81043, Italy

A novel robustness analysis technique is proposed for atmospheric re-entry applications. The problem is stated as a finite-time stability analysis of Linear-Time Varying systems on a compact time domain, subject to bounded variations in initial state and unknown parameters. The finite-time stability property is formulated as the inclusion of all the possible system trajectories into a pre-specified time-varying subset of the state space. Based on assuming the involved sets are polytopes, the proposed approach allows deducing the system finite-time stability from the property verification on a limited number of numerically computed system trajectories. An additional result is presented which allows determining a conservative estimate of the maximum norm-bound of time-varying perturbations under which the LTV system remains finite time stable. Results of the application of the proposed technique to a re-entry technology demonstrator are presented which demonstrate its effectiveness in complementing conventional LTI-based

[1] Assistant Professor, Department for Technologies, Centro Direzionale C4.
[2] Professor, Department of Aerospace Engineering, Piazzale Tecchio 80.
[3] Head, Guidance, Navigation and Control Laboratory, Via Maiorise.
[4] Head, Modelling and Simulation Laboratory, Via Maiorise.
[5] Head, Air Transport Management Laboratory, Via Maiorise.

analyses. Results also show that it is computationally viable and allows linking the system robustness to a quantitative analysis of the system trajectory dispersion around the nominal one due to concurrent initial state dispersion and uncertain parameters effects, which aids in evaluating mission objectives fulfilment.

Keywords

Robustness analysis, Linear Time Varying, Atmospheric Re-entry, Finite Time Stability

1 Introduction

The present paper proposes an original approach for advancing the current practice in Flight Control Laws (FCL) robustness analysis under parametric uncertainties for winged vehicles in the terminal gliding phases of re-entry flight. Flight dynamics of such vehicles are conventionally described by nonlinear systems evolving on a non-stationary trajectory [1]. Furthermore, the relatively low mechanical energy content of terminal flight phases, coupled to the poor gliding performances of re-entry vehicles in these flight regimes, implies that the vehicle rapidly traverses different flight conditions, and the trajectory evolves over a time interval that is typically in the order of minutes [2]. In addition, these missions are affected by significant uncertainties on some critical design parameters, most notably those related to their aerodynamic characteristics [3], implying that the FCL robustness analyses need to be continuously performed during the design cycle.

For this kind of applications, the current practice in FCL robustness analysis relies on the well-known theory of Linear Time Invariant (LTI) systems. In this approach, the original nonlinear system representing the vehicle dynamics is linearized around a limited number of representative time-varying trajectories, including the nominal one. Then, the well-known frozen-time approach [4] is applied, yielding multiple

LTI models [5]. In this way classical stability margins [6, 7] can be computed. Even if the flight experience has demonstrated that this approach is indeed operative, it is also widely recognized as inefficient [8]. In fact, LTI-based analysis may reveal poor closed-loop dynamic performances (for instance, low damping or even instabilities) in some of the chosen points on the trajectories. However, the effect of undesirable frozen-time performances on the overall mission objectives can be of scarce importance since the vehicle remains in a particular frozen time condition only for a limited amount of time. Thus, modification of the FCL for improving the LTI-based dynamic performances could be un-necessary, since these missions typically specify robustness criteria expressed as time-domain criteria, such as nominal trajectory tracking performances, which can be satisfied also in presence of poor frozen-time dynamic performances. LTI-based analysis results are thus complemented by dedicated numerical-simulation based analyses, such as Monte Carlo techniques, through which the quantitative dispersion about the reference trajectory can be estimated. Finally, in the LTI-based approach, the robustness analysis problem shall be solved in each frozen operating condition, thus considerably limiting the dimension of manageable problems due to its significant computational load.

The present paper aims at developing a robustness analysis technique capable of complementing the results of classical LTI-based analysis and overcoming its limitations, without requiring a significant computational burden. The proposed technique is intended to be used in early stages of the FCS design cycle rather than for final validation of a mature FCS design, which is usually, and successfully, performed by means of Monte Carlo analysis tools. LTI-based analyses are complemented by taking into account explicitly the time-variance of the system dynamics using Linear Time Varying (LTV) models, and focusing on robustness criteria directly linked to the dispersion of the system trajectories about the nominal one over a finite time interval. This last point is of particular importance since trajectory dispersion can provide a direct measure of the mission objectives' fulfilment.

Concerning the quantitative dispersion of the system trajectories in the state space over a finite time interval, the problem may be stated either as a reachability analysis [9, 10], or as a Finite Time Stability (FTS) analysis [11 – 13]. Even though the two theoretical frameworks bear some important similarities, there are substantial differences (see, e.g. [14]). Roughly speaking, the reachability analyses are primarily aimed at computing all the states that can be reached by a system, starting from a set of initial states, under the action of a feasible control input or disturbing signal, depending on the problem setting. On the other hand, the FTS analysis problem is concerned with the more local problem of determining conditions for which the system trajectories are guaranteed to lie within some pre-specified bounds, despite variations in initial states and disturbances. Although these are classical well known problems, the majority of the practically computable methods are concerned with LTI systems (the interested reader is referred to [9] and [11] for an overview of prominent methods), aimed at exploiting the explicit closed-form expression of the transition matrix and obtaining easily computable conditions for solving the problem. As far as LTV systems are concerned, the computation of the transition matrix is quite hard and in general requires numerical simulation. Indeed, even though most of the methods (see, e.g. [15]) can be extended with no conceptual difficulty to the LTV case, their results cannot be fully exploited, since, in order to evaluate the conditions they do provide, numerical simulation is still necessary. Thus, in the authors' opinion, for LTV systems it is advisable developing an approach which exploits the computational convenience of achieving the problem solution by the knowledge of a limited number of numerically computed system trajectories.

This paper focuses on the FTS analysis problem setting, and proposes a novel approach for LTV systems defined on a compact time interval, and subject to uncertain parametric disturbances and initial conditions varying within bounded sets, based on numerically computing a limited number of system trajectories. The proposed approach has been developed as part of the research activity on autonomous guidance, navigation and control of re-entry vehicles, carried out at the Italian Aerospace Research Centre (CIRA) within the Unmanned Space Vehicle (USV) program. This program foresees the development of Flying Test Beds

(FTBs) performing scientific experiments and technology demonstration relevant to re-entry applications, with particular concern to the terminal flight phases of re-entry manoeuvres.

The main advantage of the proposed approach is to provide a condition which is both necessary and sufficient for the FTS of such systems, based on verifying the inclusion of a finite number of numerically computed system trajectories within a prefixed time-varying subset of the state space. This condition relies on assuming all the involved sets are polytopes. Then, an extension of the proposed approach is also presented, by taking into account the effect on the LTV system's FTS of additive norm-bounded, time-varying perturbations, including system nonlinearities. In particular, a conservative estimate is provided for the maximum norm of the perturbing signals that can be added to a LTV while still preserving its FTS property. The proposed approach effectiveness and computational viability are demonstrated by showing the results of its application to the augmented longitudinal dynamics of the USV-FTB1 vehicle. In particular, a comparison with conventional LTI-based analyses is performed with the aim of highlighting the capability of the proposed approach both in complementing conventional techniques and in assessing the system robustness in terms of mission objectives' fulfilment.

2 Problem Statement

Flight dynamics of winged re-entry vehicles in terminal conditions are conventionally described by nonlinear systems evolving on a non-stationary trajectory [1]. Furthermore, the relatively low mechanical energy content of terminal flight phases, coupled to the poor gliding performances of re-entry vehicles in these flight regimes, implies that the vehicle rapidly traverses different flight conditions, during a limited, and relatively short, time interval. Taking into account time-variance and time-domain finiteness of the system trajectories is thus particularly advantageous for these applications. Let us thus refer to an LTV system of the form:

$$\dot{\boldsymbol{x}} = \mathbf{A}(t)\cdot\boldsymbol{x} + \mathbf{G}(t)\cdot\boldsymbol{\pi} \qquad \boldsymbol{x}(0) = \boldsymbol{x}_0 \tag{1}$$

where $\boldsymbol{x} \in \Re^n$ and $\mathbf{A}(\cdot) \in C^0\left([0,T], \Re^{n \times n}\right)$, that is, the dynamical matrix is defined on a compact time domain, the initial epoch is taken equal to zero for simplicity, and $\boldsymbol{\pi} \in \Re^b$ are *unknown* parametric disturbances that enter affinely the dynamical equation by means of the time-varying matrix $\mathbf{G}(\cdot) \in C^0\left([0,T], \Re^{n \times b}\right)$. The generic trajectory exists, it is unique, it continuously depends on *(t, x_0, π)*, and it can be parameterized in the initial state and unknown parameters, as follows

$$\boldsymbol{x}(t; x_0, \pi) := \boldsymbol{\Phi}(t,0) \cdot \boldsymbol{x}_0 + \left[\int_0^t \boldsymbol{\Phi}(t,\tau) \cdot \mathbf{G}(\tau)\, d\tau\right] \cdot \boldsymbol{\pi} \qquad (2)$$

Given the features of the original system dynamics, it is of interest determining quantitatively the dispersion of the trajectories (2) under expected initial state displacements and parametric uncertainties values. Among the possible frameworks in which this problem can be tackled, as recalled in the introduction, the FTS one is here taken as a reference. The present paper analyzes the FTS of the system (1), when both the initial state and the unknown parameters range in bounded sets, X_0 and Π, respectively. The FTS property requires the system trajectories to be included in a pre-fixed subset of the state space, which is referred from now on as the required solutions tube S_R. Even though the FTS concept is relatively well assessed in the relevant literature, a number of definitions can be found which differ depending on the considered input sets, their shape and time-variability. For the sake of clarity, the FTS property is specified in the present context as follows.

Definition 1 – FTS: Given the sets $X_0 \subseteq \Re^n$, $\Pi \subseteq \Re^b$, a compact time domain *[0,T]*, and a possibly time-varying set $S_R(\cdot)|_{[0,T]} \subseteq \Re^n$, if $\boldsymbol{x}_0 \in X_0, \boldsymbol{\pi} \in \Pi \Rightarrow \boldsymbol{x}(t; x_0, \pi) \in S_R(t) \quad \forall t \in [0,T]$, then the system (1) is said to be FTS with respect to $\{[0,T], X_0, S_R(\cdot), \Pi\}$.

For shorthand notation, the FTS acronym is used in the following for denoting both the finite time stability property and a finite time stable system, and the quadruple with respect to which FTS is evaluated is omitted whenever it is clearly devisable from the context.

The first problem dealt with in this paper is to verify that system (1) is FTS, once a required solutions tube is specified, as well as admissible initial state displacements and parametric disturbances.

Problem 1: Finite Time Stability Verification (FTSV): Given the sets $X_0 \subseteq \Re^n$, $\Pi \subseteq \Re^b$, and $S_R(\cdot)|_{[0,T]} \subseteq \Re^n$, determine if system (1) is FTS with respect to $\{[0,T], X_0, S_R(\cdot), \Pi\}$.

Given an FTS system, it is of interest to analyze the persistence of the FTS property in face of norm-bounded perturbations of the system dynamics. Therefore, an extension of the above problem is also considered, by taking into account the effect on system (1) of a perturbing term $\boldsymbol{d}(\cdot)$. Refer to time-varying perturbing signals, possibly nonlinearly depending on the system state and on the parametric perturbations, $\boldsymbol{d}:[0,T]\times\Re^n\times\Pi\to\Re^n$. To guarantee existence, uniqueness and continuous dependence of the system solutions on initial conditions and parameters, $\boldsymbol{d}(\cdot)$ is assumed to be continuous in $(t,\boldsymbol{x},\boldsymbol{\pi})$ and at least locally Lipschitz in $\boldsymbol{x}$ (uniformly in t and $\boldsymbol{\pi}$) on an open and connected set $D \subseteq \Re^n$, such that $S_R(t) \subseteq D \quad \forall t \in [0,T]$. In addition, assume the $\boldsymbol{d}(\cdot)$ function to be norm-bounded by a finite positive constant γ.

$$\dot{\boldsymbol{x}}_d = \mathbf{A}(t)\cdot\boldsymbol{x}_d + \mathbf{G}(t)\cdot\boldsymbol{\pi} + \boldsymbol{d}(t,\boldsymbol{x}_d,\boldsymbol{\pi}) \qquad \boldsymbol{x}_d(0) = \boldsymbol{x}_0 \tag{3}$$

$$\gamma \in \Re:\ 0<\gamma<\infty,\ \left\|\boldsymbol{d}(\cdot,\boldsymbol{x},\boldsymbol{\pi})\right\|_\infty \le \gamma \quad \forall \boldsymbol{x}\in\Re^n, \forall \boldsymbol{\pi}\in\Pi \tag{4}$$

The term $\boldsymbol{d}(\cdot)$ may represent plant uncertainty, modeling errors, model nonlinearity, or, in case the dependency on x is dropped, exogenous non-parametric disturbances. The trajectories of the system (3), referred as the *perturbed* system, are the solutions of the following implicit integral equation.

$$\boldsymbol{x}_d(t;\boldsymbol{x}_0,\boldsymbol{\pi}) := \boldsymbol{\Phi}(t,0)\cdot\boldsymbol{x}_0 + \int_0^t \left\{\boldsymbol{\Phi}(t,\tau)\cdot\left[\mathbf{G}(\tau)\cdot\boldsymbol{\pi} + \boldsymbol{d}(\tau,\boldsymbol{x}_d,\boldsymbol{\pi})\right]\right\} d\tau \tag{5}$$

The problem of verifying the persistence of FTS property in face of the introduced perturbing term is here stated as to analyze to which extent a FTS system may be perturbed while still remaining FTS. This maximum value of the perturbing signal's norm bound may be interpreted as a robustness margin of the FTS property w.r.t. perturbations, which is defined as follows.

$$\tilde{\gamma} := \sup\left\{\gamma \mid (3) \text{ is FTS w.r.t. } \left\{[0,T], X_0, S_R(\cdot), \Pi\right\}\right\} \quad (6)$$

In this perspective, the problem of determining the robustness margin γ□ for a given FTS system is introduced as follows.

Problem 2: Robustness Margin Determination (RMD): Given the sets $X_0 \subseteq \Re^n$, $\Pi \subseteq \Re^b$, $S_R(\cdot)|_{[0,T]} \subseteq \Re^n$, and a system (1), which is FTS with respect to $\{[0,T], X_0, S_R(\cdot), \Pi\}$, determine the robustness margin (6).

3 Solution Approach

As discussed in the introduction, several methods exist for determining the FTS of a linear system, either using methods developed in the FTS analysis framework, or taking advantage of techniques from reachability analysis. Nonetheless, most of the literature on FTS analysis and computation of the reachable sets is devoted to the case of linear time–invariant systems, in order to exploit the explicit closed-form expression of the transition matrix and to obtain easily computable conditions for solving the problem. As far as LTV systems are concerned, the computation of the transition matrix is quite hard and in general requires simulation, thus all the former methods cannot be fully exploited, because numerical simulation of the system is necessary for evaluating the conditions they do provide. Thus, for LTV systems, it makes sense to adopt an approach that takes into account that numerical simulation shall be employed in any case. In the authors' opinion, for LTV systems it is convenient to exploit some basic, well-known properties of linear systems that allow inferring the FTS property of the system from those of a limited number of its trajectories, which can be obtained by numerical simulation. In order for this approach to be feasible from a practical perspective, this paper focuses on the case in whom both initial states and parametric uncertainties belong to polytopic sets.

Let us assume henceforth that all the sets involved in Definition 1 are polytopes. The definition and discussion of notions about polytopes are omitted for brevity, since they are well-known and easily available in the open literature (the reader is referred to [16] for a comprehensive treatment of the subject). Only one of the fundamental properties of a polytope in $\Re^n$ is recalled here, that is, that it can be described

either as an intersection of a finite number m of closed half-spaces, $P := \{\boldsymbol{x} \in \Re^n \mid \mathbf{P}^H \boldsymbol{x} \leq \boldsymbol{P}^K\}$, where $\mathbf{P}^H \in \mathcal{R}^{m \times n}$, $\boldsymbol{P}^K \in \mathcal{R}^{m \times 1}$, or described by its v_P vertices, as

$$P = \left\{ \boldsymbol{x} \in \Re^n \;\middle|\; \boldsymbol{x} = \sum_{i=1}^{v_P} \alpha_i \boldsymbol{x}^{(i)},\ \alpha_i \geq 0,\ \sum_{i=1}^{v_P} \alpha_i = 1 \right\}$$

The Minkowski-Weyl theorem [16] tells us the two representations are equivalent from a theoretical perspective, and are commonly referred to as $\mathcal{H}$ and $\mathcal{V}$–representation. However, changing the polytope representation may often be computationally unfeasible [17], implying that the two representation should be considered as distinct for practical purposes. Let us also introduce some assumptions on the representations of the polytopes involved in Definition 1, so to retain simplicity in exposition, but which don't alter the results of the paper.

Assumption 1. The initial state displacements range in a polytope X_0, which is given in minimal $\mathcal{V}$–representation as

$$X_0 = \left\{ \boldsymbol{x}_0 \in \Re^n \;\middle|\; \boldsymbol{x}_0 = \sum_{i=1}^{v_0} \theta_i \boldsymbol{x}_0^{(i)},\ \theta_i \geq 0,\ \sum_{i=1}^{v_0} \theta_i = 1 \right\}$$

Assumption 2. The unknown parameters range in a polytope Π, which is given in minimal $\mathcal{V}$–representation as

$$\Pi = \left\{ \boldsymbol{\pi} \in \Re^b \;\middle|\; \boldsymbol{\pi} = \sum_{i=1}^{v_\pi} \lambda_i \boldsymbol{\pi}^{(i)},\ \lambda_i \geq 0,\ \sum_{i=1}^{v_\pi} \lambda_i = 1 \right\}$$

Assumption 3. The required solutions tube is a full-dimensional polytope for all $t \in [0,T]$, which is given in minimal $\mathcal{H}$–representation, normalized w.r.t. the 2 – norm, as

$$S_R(t) := \left\{ \boldsymbol{x} \in \Re^n \;\middle|\; \mathbf{S}^H(t) \cdot \boldsymbol{x} \leq \boldsymbol{S}^K(t) \right\} \qquad (7)$$

where $\mathbf{S}^H(\cdot) \in C^0([0,T], \Re^{m\times n})$, $\boldsymbol{S}^K \in C^0([0,T], \Re^{m\times 1})$.

In general, both the FTSV and RMD problems can be reduced to that of estimating the reachable set of an autonomous augmented system in the presence of bounded disturbances. System (3) can be indeed recast as

$$\begin{bmatrix} \dot{\boldsymbol{x}}_d \\ \dot{\boldsymbol{\pi}} \end{bmatrix} = \begin{bmatrix} \mathbf{A}(t) & \mathbf{G}(t) \\ 0 & 0 \end{bmatrix} \cdot \begin{bmatrix} \boldsymbol{x}_d \\ \boldsymbol{\pi} \end{bmatrix} + \begin{bmatrix} \boldsymbol{d}(t, \boldsymbol{x}_d, \boldsymbol{\pi}) \\ 0 \end{bmatrix}$$

thus reducing to $d\boldsymbol{z}/dt = \mathbf{A}_{Aug}(t)\boldsymbol{z}+\boldsymbol{d}_{Aug}$, with $\boldsymbol{z} = (\boldsymbol{x}_d{}^{\mathrm{T}}, \boldsymbol{\pi}^{\mathrm{T}})^{\mathrm{T}}$ originating in the polytope $Z_0 := X_0 \times \Pi$. It is obvious that for $\boldsymbol{d} = 0$ the augmented state evolution $\boldsymbol{z}(t)$ will be inside the polytope $Z(t)$ defined by the trajectories originated from the vertices of Z_0. Therefore the nominal finite state stability is easily determined from numerical simulation of a limited number of trajectories. Indeed, $\boldsymbol{x}(t)$ is confined in the relevant projection of $Z(t)$, which is a polytope denoted as the solutions tube $S(t)$, i.e. $S(t) := \{\boldsymbol{x}(t;\boldsymbol{x}_0,\boldsymbol{\pi}) \in \Re^n \mid \boldsymbol{x}_0 \in X_0, \boldsymbol{\pi} \in \Pi\}$. As such, given the polytopes X_0, Π, and $S_R(\cdot)|_{[0,T]}$, system (1) is FTS w.r.t. $\{[0,T], X_0, S_R(\cdot), \Pi\}$ if and only if $\forall t \in [0,T]$, $\forall i \in \{1,\ldots,v_0\}$, $\forall j \in \{1,\ldots,v_\pi\}$ $\boldsymbol{x}(t;\boldsymbol{x}_0{}^{(i)},\boldsymbol{\pi}^{(j)}) \in S_R(t)$.

The FTSV problem solution can be obtained with no conservatism from the FTS property verification on a finite (and known a priori) number of its trajectories. The $v_0 \cdot v_\pi$ trajectories to be checked are the system solutions under all the possible combinations of vertex values of the initial state and parameters polytopic domains. In the present work, the authors propose to accomplish the inclusion check by obtaining the needed trajectories numerically, as specified in section 3.1. Therefore, the FTSV problem can be solved numerically as far as its solution remains computationally viable, as it is shown in section 4.

In general, some of the points $\boldsymbol{x}^{(i)}(t)$ may not be vertices of $S(t)$. This implies that system (1) FTS property can be proved to be equivalent also to the inclusion in $S_R(t)$ only of the points effectively being vertices of $S(t)$, allowing to check a smaller number of trajectories. However, the latter alternative might

well be computationally inconvenient, because determining the vertices of *S(t)* requires solving a series of linear programming problems in *n* variables and $v_0 \cdot v_\pi$ constraints [18], which call for a non-negligible amount of additional computations.

The effects of the perturbing term ***d(·)*** on the dynamical equation are now taken into account. Under the assumption $\|\boldsymbol{d}\|_\infty < \gamma$, it is well-known that the vector $z(t)$ originating from Z_0 is included in the set $Z(t) \oplus O(t)$, where $Z(t)$ is defined, as stated before, by the vertex trajectories, and $O(t)$ is the 0–reachable set under bounded disturbances. Then the problem, basically, could be solved determining the 0–reachable set with bounded input. This is a classic problem, well established in the literature, intensively studied in the 70s–80s (see [9] for an overview of the prominent results). For the previously discussed reasons, basic properties of linear systems are exploited also in this case, taking explicitly into account that knowledge of a finite number of trajectories is available by means of numerical simulations. This allows deriving in the following a proposition that yields a conservative estimate of the FTS robustness margin γ□. This proposition follows the most popular approaches for determining 0-reacheable sets of LTI systems, such as 15, but avoiding to exploit the closed-form expression of the transition matrix. In order to state it, two claims must be first discussed. First, a result is provided that allows to conservatively bound the perturbed system's solutions tube. Let us assume from now on that the $\mathcal{V}$–representation of *S(t)* is available, since the RMD problem makes sense only once the system's FTS has already been ascertained, and define the solutions tube $S_d(t)$ relative to the perturbed system (3) as:

$$S_d(t) := \left\{ \boldsymbol{x}_d(t; \boldsymbol{x}_0, \boldsymbol{\pi}) \in \Re^n \,\middle|\, \boldsymbol{x}_0 \in S_0, \boldsymbol{\pi} \in \Pi \right\} \tag{8}$$

The tube (8) can be bounded by augmenting system (1) solutions tube with a B_r of an opportune radius, given by the following claim.

Claim 1: Consider the polytopes X_0, $S_R(\cdot)|_{[0,T]}$, and Π. Consider the perturbed system (3), subject to perturbations complying with (4). Define the functions $r_1(t) := \int_0^t \left|\boldsymbol{\Phi}(t,\tau)\right|_\infty d\tau$ and $r(t) := r_1(t) \cdot \gamma$.

Then $S_d(t) \subseteq S(t) \oplus B_{r(t)}$, $\forall t \in [0,T]$.

Proof. Let us refer to the difference between the systems solutions with and without the perturbing term $\boldsymbol{d}$, (2), and (5), introducing the variable $\boldsymbol{\xi}(t;\boldsymbol{\pi}) := \boldsymbol{x}_d(t;\boldsymbol{x}_0,\boldsymbol{\pi}) - \boldsymbol{x}(t;\boldsymbol{x}_0,\boldsymbol{\pi})$. The $\boldsymbol{\xi}$ dynamics are described by the following differential equation, in which the initial condition is always identically zero.

$$\dot{\boldsymbol{\xi}} = \mathbf{A}(t)\cdot\boldsymbol{\xi} + \boldsymbol{d}(t,\boldsymbol{x}_d,\boldsymbol{\pi}) \qquad \boldsymbol{\xi}(0;\boldsymbol{\pi}) = 0 \tag{9}$$

The trajectories of (9) may be implicitly expressed as the solutions of the integral equation. $\boldsymbol{\xi}(t;\boldsymbol{\pi}) = \int_0^t \boldsymbol{\Phi}(t,\tau)\cdot\boldsymbol{d}(\tau,\boldsymbol{x}_d,\boldsymbol{\pi})\,d\tau$. Clearly it follows that $\left|\boldsymbol{\xi}(t;\boldsymbol{\pi})\right|_\infty \le \int_0^t \left|\boldsymbol{\Phi}(t,\tau)\cdot\boldsymbol{d}(\tau,\boldsymbol{x}_d,\boldsymbol{\pi})\right|_\infty d\tau$. Given the induced infinity norm properties, it also follws that $\left|\boldsymbol{\Phi}(t,\tau)\cdot\boldsymbol{d}(\tau,\boldsymbol{x}_d,\boldsymbol{\pi})\right|_\infty \le \left|\boldsymbol{\Phi}(t,\tau)\right|_\infty \cdot \left|\boldsymbol{d}(\tau,\boldsymbol{x}_d,\boldsymbol{\pi})\right|_\infty$ for any two time epochs t and τ, $t \ge \tau$. Thus $\left|\boldsymbol{\xi}(t;\boldsymbol{\pi})\right|_\infty \le \left[\int_0^t \left|\boldsymbol{\Phi}(t,\tau)\right|_\infty d\tau\right]\cdot\gamma$, which is equivalent to $\boldsymbol{\xi}(t;\pi) \in B_{r(t)}$, $\forall \pi \in \Pi$, $\forall t \in [0,T]$. Hence, since $\boldsymbol{\xi}(t;\pi)$ belongs to $B_{r(t)}$ whatever the value of $\boldsymbol{\pi}$ in Π, $\boldsymbol{x}_d(t;\boldsymbol{x}_0,\boldsymbol{\pi})$ will belong to the Minkowski sum of $B_{r(t)}$ and of system (1) solutions tube, thus concluding the proof.

Claim 1 allows to conservatively estimate the tube in which the trajectories lie when the system is perturbed by whatever $\boldsymbol{d}(\cdot)$, provided that the perturbation is norm-bounded in the sense of (4). In order to take advantage of claim 1 in solving the RMD problem, the following claim establishes an estimate of the maximum radius of a B_r that can be added, in the Minkowski sense, to $S(t)$ still resulting into a tube included in $S_R(t)$ (explicit time dependency is omitted in this claim for notational compactness).

Claim 2: Consider the two polytopes S and S_R. Let $S \subseteq S_R$. Define the function $\bar{r}:[0,T] \to \Re$ as $\bar{r} = \min_{\substack{i=1,\ldots,v_0 v_\pi \\ j=1,\ldots,m}} \left[S_j^K - \boldsymbol{S}_j^H \boldsymbol{x}^{(i)}\right]$, where $\boldsymbol{S}_j^H$ and S_j^K stand for the j-th row of the matrices introduced in Eq.(7). The following hold.

(i) $r \le (n)^{-1/2}\,\bar{r} \;\Rightarrow\; S \oplus B_r \subseteq S_R$

(ii) $S \oplus B_r \subseteq S_R \Rightarrow r \le \bar{r}$

(iii) If S_R is hyper-rectangular, then $r \le \bar{r} \;\Leftrightarrow\; S \oplus B_r \subseteq S_R$

Proof. To prove (i), let us consider the *j*-th facet of S_R, and take the absolute value of the vector inner product of its outward normal versor and a generic vector $\boldsymbol{z}$ in $\Re^n$. Applying Cauchy – Schwarz inequality and the properties of *p*-norms yields $\left|\left\langle \left(\boldsymbol{S}_j^H\right)^T, \boldsymbol{z} \right\rangle\right| \le \left|\left(\boldsymbol{S}_j^H\right)^T\right|_2 |\boldsymbol{z}|_2 \le \sqrt{n}\,|\boldsymbol{z}|_\infty$. Thus, if $\boldsymbol{z} \in B_r$, the following holds for all *m* facets.

$$\left|\left\langle \left(\boldsymbol{S}_j^H\right)^T, \boldsymbol{z} \right\rangle\right| \le \min_{\substack{i=1,\ldots,v_0 v_\pi \\ j=1,..,m}} \left[S_j^K - \boldsymbol{S}_j^H \boldsymbol{x}^{(i)} \right] \qquad (10)$$

Considering that an affine function attains its minimum over a polytope at a vertex, the above inequality can be exploited to obtain the weaker condition $\left\langle \left(\boldsymbol{S}_j^H\right)^T, \boldsymbol{z} \right\rangle \le S_j^K - \boldsymbol{S}_j^H \boldsymbol{x}$, $\forall \boldsymbol{x} \in S$,. $\forall \boldsymbol{z} \in B_r$, $\forall j = 1,\ldots,m$. It is straightforward to verify that the above is equivalent to $S \oplus B_r \subseteq S_R$, thus proving (i).

The (ii) statement may be proved by contradiction. Let us consider a radius $r > \bar{r}$, and denote as $\bar{i}, \bar{j}$ the couple of indices minimizing the $\bar{r}$ function, that is, $\exists\left(\bar{i}, \bar{j}\right) \in \{1,..,v_0 v_\pi\} \times \{1,..,m\}$: $S_{\bar{j}}^K - \boldsymbol{S}_{\bar{j}}^H \boldsymbol{x}^{(\bar{i})} = \bar{r}$. Taking $\bar{\boldsymbol{z}} = r \cdot \left(\boldsymbol{S}_{\bar{j}}^H\right)^T$, it is trivial to verify that $\bar{\boldsymbol{z}} \in B_r$. Because $\left\langle \left(\boldsymbol{S}_{\bar{j}}^H\right)^T, \bar{\boldsymbol{z}} \right\rangle = r$, one obtains $\boldsymbol{S}_{\bar{j}}^H \left(\boldsymbol{x}^{(\bar{i})} + \bar{\boldsymbol{z}}\right) - S_{\bar{j}}^K = r - \bar{r} > 0$, which contradicts the initial assumption that $S \oplus B_r \subseteq S_R$.

At last, given (ii), one must only prove necessity in (iii). Necessity may be shown following the proof of (i). Again, let us consider the *j*-th facet of S_R, and take the absolute value of the vector inner product of its outward normal versor and a generic vector $\boldsymbol{z}$ in $\Re^n$. Because S_R is hyper-rectangular, the versor $\left(\boldsymbol{S}_j^H\right)^T$ is equal to $\pm\boldsymbol{e}_k$ for some $1 \le k \le n$, i.e., the *k*-th column of the $n \times n$ identity matrix. The inner product of

$\left(\boldsymbol{S}_j^H\right)^T$ and $\boldsymbol{z}$ is thus equal to ± the *k*-th component of $\boldsymbol{z}$. The condition $\left|\left\langle\left(\boldsymbol{S}_j^H\right)^T, \boldsymbol{z}\right\rangle\right| \le |\boldsymbol{z}|_\infty$ is thus trivial. Hence, Eq.(10) holds under condition $r \le \bar{r}$ this time, and the proof may proceed as for (i).

Claim 2 identifies the maximum dispersion in the state space that can be added to the solutions of system (1) while still remaining FTS. Under assumptions 1–3, this dispersion may be conservative, but at most of a bounded (and known a priori) amount, in the sense that it might exist a $B_r : S \oplus B_r \subseteq S_R$, with a radius higher than the one specified by (i), but at most equal to $\bar{r}$. Nonetheless, if the required solutions tube is hyper-rectangular at a certain time epoch, condition (iii) allows to sharpen the radius bound (i) as to obtain the maximum radius under which inclusion in S_R is preserved, and thus to avoid any conservatism.

The main result can now be stated for the RMD problem solution, which follows almost immediately from the previous claims.

Proposition 1: Consider the sets $X_0 \subseteq \Re^n$, $\Pi \subseteq \Re^b$, $S_R(\cdot)|_{[0,T]} \subseteq \Re^n$, and a system (1) FTS with respect to $\{[0,T], X_0, S_R(\cdot), \Pi\}$. Define $\bar{\gamma} \in \Re_+$ as $\bar{\gamma} := \min_{t \in [0,T]} \bar{r}(t) / r_1(t)$. System (3) is FTS with respect to $\{[0,T], X_0, S_R(\cdot), \Pi\}$ if $\left\|\boldsymbol{d}(\cdot, \boldsymbol{x}, \boldsymbol{\pi})\right\|_\infty \le (n)^{-1/2} \cdot \bar{\gamma} \;\; \forall \boldsymbol{x} \in \Re^n, \forall \boldsymbol{\pi} \in \Pi$. In case S_R is hyper-rectangular at each time epoch in $[0,T]$, the result holds for $\left\|\boldsymbol{d}(\cdot, \boldsymbol{x}, \boldsymbol{\pi})\right\|_\infty \le \bar{\gamma} \;\; \forall \boldsymbol{x} \in \Re^n, \forall \boldsymbol{\pi} \in \Pi$.

Proposition 1 provides a conservative solution to the RMD problem, because of the conservatism introduced by the previous claims. The upper bound on the perturbing signal norm obtained by Proposition 1 may be, in general, smaller than the robustness margin γ□. A quantitative example of the amount of introduced conservatism is given in section 4.

3.1 Algorithmic Application

The results obtained in this section can be verified in a computationally efficient manner, taking advantage of very well-known results in linear systems. A brief sketch of the main steps required for

computing the solution to the FTSV and RMD problems is provided in the following, for the sake of completeness.

Taking advantage of the previous remarks, the FTSV problem may be solved by checking the inclusion of a limited number of trajectories (2) in the required solutions tube. The approach proposed in this paper obtains these trajectories numerically. Following immediately from linear system's properties, the generic trajectory of system (1) is obtained as a linear combination of *(n+b)* trajectories, computed by numerical simulations. Indeed the *n* columns of $\boldsymbol{\Phi}(\cdot,0)$ are the *n* solutions of Eq.(1) under $\boldsymbol{\pi}=0$ and initial conditions $\boldsymbol{x}_{i0} = \boldsymbol{e}_i$ *(i=1, . . . , n)*, and the *b* columns of $\mathbf{M}(t) := \int_0^t \boldsymbol{\Phi}(t,\tau)\cdot\mathbf{G}(\tau)\,d\tau$ are the *b* solutions with zero initial condition and taking the uncertain parameters as the standard basis of $\Re^b$, i.e. $\boldsymbol{\pi}_i = \boldsymbol{e}_i$ *(i=1, . . . , b)*. These two time-varying matrices are thus computed by numerical simulations of the above mentioned *(n+b)* solutions. This is done discretizing the problem by partitioning the time interval *[0,T]*. For the sake of simplicity, refer henceforth to a uniform partition $0=t_0, t_1, \ldots, t_{Ns} = T$ of the time interval *[0,T]*, with N_S subintervals and a mesh Δt, even though all the results presented in this section may be easily extended to other kinds of partitions. In this way, the values of $\boldsymbol{\Phi}(t_k,0)$ and $\mathbf{M}(t_k)$, $k = 1, \ldots, N_S$, can be obtained by employing the *(n + b)* values of the above mentioned solutions. Then, the FTSV problem may be solved exactly first obtaining at each t_k the $v_0 \cdot v_\pi$ trajectories necessary for establishing the FTS, by applying the linear transformations in (2), and then checking the validity of the *m* linear inequalities (7).

Solution of the RMD may be achieved once the FTSV has been solved. In this case, indeed, at each t_k, $\bar{r}$ can be computed by exhaustive minimization of the $S_j^K - \boldsymbol{S}_j^H \boldsymbol{x}^{(i)}$ scalar function over the *m* facets of S_R and $v_0 \cdot v_\pi$ points of the $\mathcal{V}$–representation of *S*. In order to compute r_1, an approximate numerical procedure has been designed, in which the integral is substituted by the Riemann sum corresponding to the uniform partition $t_0, \ldots, t_{Ns}$. The Riemann sum involves terms of the form $|\boldsymbol{\Phi}(t_k,t_i)|_\infty$, to be computed for all t_k ($0 \le k \le N_S$) and all t_i ($0 \le i \le k-1$). The generic $|\boldsymbol{\Phi}(t_k,t_i)|_\infty$ can be obtained by making use of the semi-group

property as $|\mathbf{\Phi}(t_k,t_i)|_\infty = \left|\prod_{j=i+1}^{k} \mathbf{\Phi}\left(t_j,t_{j-1}\right)\right|_\infty$, and each $\mathbf{\Phi}(t_j,t_{j-1})$ can be determined by employing numerical simulations. First, the following time varying matrix is computed at each t_j by n opportune numerical simulations, similarly to what has been done in the FTSV solution context, $\mathbf{F}\left(t_j\right) := \int_0^{t_j} \mathbf{\Phi}\left(t_j,\tau\right) d\tau$. Then, the values of $\mathbf{F}(t_j)$ are used to obtain the $\mathbf{\Phi}(t_j,t_{j-1})$, employing the relationship $\mathbf{\Phi}\left(t_j,t_{j-1}\right) \cong \mathbf{F}\left(t_j\right) \cdot \left[\Delta t \cdot \mathbf{I} + \mathbf{F}\left(t_{j-1}\right)\right]^{-1}$. Finally, $\bar{\gamma}$ may be computed by exhaustive minimization of the ratio between $\bar{r}$ and r_1 over the partition $t_0, \ldots, t_{Ns}$.

4 Application to FTB1 longitudinal dynamics

4.1 FTB1 Longitudinal Dynamics Model

This section introduces the nonlinear system describing the closed-loop longitudinal flight dynamics of the experimental reusable launch vehicle demonstrator USV-FTB1 [19] currently operated by the CIRA. The FTB1 vehicle is the first of three planned vehicle configurations that CIRA is developing as part of its USV Program, whose main goal is contributing to the international community effort toward the development of next generation reusable space vehicles. This vehicle is planned to execute flight tests in subsonic, transonic and low supersonic flight regimes, in view of the development of upgraded vehicle configurations to perform sub-orbital and orbital re-entry flights. The FTB1 vehicle, shown in Fig. 1, is unmanned and un-powered. It has a slender wing configuration, with two sets of aerodynamic effectors: the elevons, which provide pitch control when deflected symmetrically and roll control when deflected asymmetrically, and the rudders for yaw control.

The first FTB1 mission is specifically considered to show the effectiveness of the proposed technique. It foresees a drop of the vehicle from a stratospheric balloon (at nearly null velocity and angle of attack) to reach Mach numbers above 1.0 for investigating aerodynamics and advanced guidance navigation and

control in the transonic phase of an un-powered re-entry flight. The basic operations of the mission, sketched in Fig. 2, consist of an ascent phase during which the stratospheric balloon brings the FTB1 at the release altitude of about 20Km followed by a flight phase where the FTB1 is dropped and the aerodynamic controlled flight starts. The vehicle achieves the transonic flight conditions at an altitude between 10 and 15 km; then it starts a slow down manoeuvre (up to 0.6 Mach) at the end of which a recovery parachute is opened. The mission ends with the demonstrator splash down in the Mediterranean sea. Mission and GNC system requirements for the first mission of the FTB1 vehicle are listed in Table 1.

The open-loop nonlinear dynamical function arises from the standard nonlinear longitudinal equations of motion, whose expression is given below and relevant assumptions can be found in [20].

$$\dot{V} = -\left(\frac{\Sigma}{m_v}\right) q_\infty C_D^{Tr} + g\sin(\alpha - \theta) \qquad (11a)$$

$$\dot{\alpha} = -\left(\frac{\Sigma}{m_v}\right)\left(\frac{q_\infty}{V}\right) C_L^{Tr} + q + \left(\frac{g}{V}\right)\cos(\alpha - \theta) \qquad (11b)$$

$$\dot{q} = \left(\frac{\Sigma c}{I_{yy}}\right) q_\infty C_m^{Tr} \; ; \qquad \dot{h} = V\sin(\theta - \alpha) \qquad (11c, d)$$

$$\dot{R} = V\cos(\theta - \alpha); \qquad \dot{\theta} = q \qquad (11e, f)$$

According to the FTB1 complete aerodynamic dataset, which is presented in [21], the lift, drag and pitching moment coefficients are the sum of a nominal and an uncertain aliquot. The former is obtained by interpolation of data given at discrete points of the flight envelope, depending on α, h, q, M, and the symmetric deflection of the elevons. In the present application, the influence of uncertainties on the relevant aerodynamic coefficient is modeled by means of non-dimensional scaling functions $s(\cdot)$ that depend on the Mach number, which multiply a non-dimensional uncertain parameter. The scaling functions are taken, for simplicity, equal to the 2σ uncertainty range at each Mach number, also allowing normalizing to [-1,1] the

uncertain parameters ranges. The uncertain parameters vector comprises the major uncertainties in the longitudinal aerodynamic coefficients [22] yielding $\boldsymbol{\pi}$:=(π_{L0} π_{D0} $\pi_{D\alpha}$ π_{m0} $\pi_{m\alpha}$ $\pi_{m\delta}$)$^{\mathrm{T}}$. The resulting aerodynamic coefficients functional dependencies are given in the following equations:

$$C_L^{Tr} = C_L(\alpha, M, h, q, \delta_e) + s_{L0}(M)\pi_{L0} \tag{12a}$$

$$C_D^{Tr} = C_D(\alpha, M, h, \delta_e) + s_{D0}(M)\pi_{D0} + \alpha^2 s_{D\alpha}(M)\pi_{D\alpha} \tag{12b}$$

$$C_m^{Tr} = C_m(\alpha, M, h, q, \delta_e) + s_{m0}(M)\pi_{m0} + \alpha s_{m\alpha}(M)\pi_{m\alpha} + \delta_e s_{m\delta}(M)\pi_{m\delta} \tag{12c}$$

The vehicle dynamics are augmented by a flight control law embedded in the vehicle Flight Control System (FCS), which is composed by the software dedicated to the measurement acquisition and by the one for computating the proper actuator commands to safely perform the mission. By considering only the functional interfaces, the FCS software, which is hosted on the Guidance, Navigation and Control on Board Computer (GNC-OBC) is linked to the Integrated inertial/satellite Measurement System (IMS) for measurement/housekeeping data acquisition and unit configuration, the Air Data Computer (ADC) for air data measurement acquisition, the Actuators Interface System (AIS) for actuators positions measurement acquisition and actuators command generation, and the Data Handling on Board Computer (DH-OBC), where vehicle and mission management is performed, for data, status and commands exchange. The FCS functional architecture is shown in Fig. 3. The FCS implements a proportional-derivative flight control law, shown in Fig. 4, arranged in a cascade structure with feedback on pitch rate and angle of attack. The augmented vehicle is driven by a time-varying angle of attack reference signal α_{ref}, which ramps up from zero at the vehicle release from the stratospheric balloon up to 7 deg. before reaching transonic conditions, value to be maintained for the remainder of the mission. The overall feedback action can be expressed as follows:

$$\delta_e = k_3\left[k_1(\alpha_{ref} - \alpha) + \zeta - q\right]; \qquad \dot{\zeta} = k_1 k_2(\alpha_{ref} - \alpha) \tag{13}$$

Two of the three gains of the controller, k_1, k_2, and k_3 are scheduled depending on the dynamic pressure q_∞, according to $k_1 = k_{10}$, $k_2 = k_{20} + k_{2s}\, q_\infty$, and $k_3 = k_{30} + k_{3s}/q_\infty$. The control law algorithm is implemented in MATLAB/SIMULINK environment and the real time code is produced by using rapid prototyping techniques and tools for automatic program building.

The complete nonlinear system to be linearized is obtained composing the aerodynamic coefficients model of Eq. (12) with the open-loop longitudinal dynamics of Eq.(11), in which δ_e is given by Eq. (13) and the open-loop state is augmented by ζ. The system has thus a seven dimensional state vector, i.e. n=7, subject to the above mentioned six dimensional vector of unknown parameters, i.e. b=6.

The state vector of all linear models presented in the following is defined in terms of variations with respect to the nominal time-varying trajectory $\tilde{\boldsymbol{z}}(\cdot)\big|_{[0,T]}$ (see [22] for a description), i.e. $\boldsymbol{x} := \boldsymbol{z} - \tilde{\boldsymbol{z}}$, where $\boldsymbol{z}$:= $(V\ \alpha\ q\ h\ R\ \theta\ \zeta)^{\mathrm{T}}$. All analysis are carried out starting from 12 s. after the vehicle release (taken as the initial time $t_0 = 0$), because it corresponds to the flight phase in whom the elevons gain a sufficient command authority, and end for $T \approx 61$ s, since the USV-FTB1 demonstrator's first mission lasts about 73 s.

The numerical results presented in this section are restricted to the case in which the uncertain parameters range in a b-hyper-rectangle in $\mathfrak{R}^b$, which can be obtained as the Cartesian product of b closed intervals in $\mathfrak{R}$. Hyper-rectangles are frequently used in practical engineering problems, and a b-hyper-rectangular Π would result when the b parameters are representative of independent aerodynamic uncertainties, which is also the commonly employed assumption when performing LTI-based stability analyses under parametric uncertainties (see, e.g. [19, 7]). More precisely, Π refers to the case of 2σ uncertainty ranges on the aerodynamic coefficients. Given the aerodynamic model of Eq. (12), Π is obtained by a uniform scaling of the unit b-hypercube with a scale factor equal to 2, and it is translated as to be symmetrical about the origin, i.e. $\Pi = [-1, 1]^b$. Additional results are shown with the uncertain parameters varying in their 1σ ranges, which yields $\boldsymbol{\pi} \in \Pi' = 0.5 \cdot \Pi$.

4.2 Conventional LTI Stability Analysis

The stability properties of the system are first examined by means of the analysis methods used in the current industrial practice for space applications, which mainly relies on the theory of LTI systems. Thus, the original nonlinear system is linearized at N_{LIN} epochs of the nominal time-varying trajectory. Specifically, 62 linearization epochs, uniformly distributed in the time interval $[0,T]$, are considered. The state vector of the N_{LIN} LTI systems does not include the variable R, since it does not influence the other vehicle states and, in addition, it is not relevant to the stability analysis of the vehicle dynamics. For each linearization epoch, the well-known frozen-time approach is applied, yielding multiple LTI models. In fact, the linearization is performed by first order expansion of the nonlinear dynamics around $\boldsymbol{x} = 0$ and for different values of the uncertain parameters, representing nominal (null π) and off-nominal conditions, obtained by evaluating the uncertain system parameters at N_{unc} points of the uncertainty parameter space Π. Specifically, the considered off-nominal systems are obtained by evaluating the uncertain parameters at all the 2^b vertices of Π, that is at N_{unc}=64 points.

Classical stability criteria can be then applied to the LTI systems. Specifically, the maximum real part of the eigenvalues associated to the 65 LTI dynamic matrices corresponding to each frozen-time epoch (one for the nominal system and 64 for the off-nominal LTI systems) is evaluated. The results presented in Table 2 refer, respectively, to the cases of 2σ (uncertainty space denoted as Π) and 1σ (uncertainty space denoted as $\Pi' = 0.5 \cdot \Pi$) uncertainty ranges in the aerodynamic coefficients. The unstable epochs, for both uncertainty ranges, are the ones marked on the nominal Mach and angle of attack plots in Fig. 5. On a standard desktop PC equipped with a Pentium IV 2.4 GHz processor and 2GB RAM, the execution time is about 21 seconds for one-epoch stability analysis and about 1260 seconds for the analysis of all the considered 62 linearization epochs.

From Table 2 it can be seen that, in both the examined cases, the linearized uncertain system is unstable at least in one point of the nominal trajectory. Nevertheless, no information can be inferred on how and if

the local (frozen-time) stability affects the non linear system behaviour and which is its impact on mission objective fulfilment. Indeed, since the vehicle rapidly changes its flight condition, observed instabilities may have negligible effects on the vehicle behaviour with respect to the nominal trajectory. Moreover, as remarked in the introduction, the conventional LTI analysis requires the introduction of fictitious equilibrium points, obtained by the frozen-time approach. Even if the flight experience has demonstrated that this approach is indeed operative, its effectiveness for re-entry mission analysis is questionable, because the nominal trajectory may not be an equilibrium trajectory for the non linear system in off-nominal conditions. Therefore, the frozen-time analysis can provide only indicative, and often heavily conservative, results. Based on these results one is forced to improve the FCL design to correct for observed local instabilities without introducing appreciable improvements in the mission execution, but on the contrary increasing control algorithm complexity and/or degrading control performance.

4.3 Proposed LTV-based FTS Analysis

This section presents the results of application of the approach proposed in the paper. The time varying matrices in (1) are obtained by first order expansion of the nonlinear dynamics around $\boldsymbol{x} = 0$, $\boldsymbol{\pi} = 0$, and are recast in a non dimensional form by introducing the weight vector $\boldsymbol{w}$:= (10 m/s, 5 deg, 5 deg, 1km, 1km, 5 deg, 10 deg/s)^T . The analysis is carried out by sampling the trajectory time span [0 s, 61s] with a uniform partition of $N_S = 190$ samples.

As previously discussed, the solution of the FTSV problem (and thus also of the RMD) requires an algorithm whose computational complexity largely depends on the number of vertices of the input polytopes, v_0 and v_π as well as the number of the required solutions tube's facets, m. These quantities may vary tremendously depending on the kind of polytopes considered. Because of their frequent occurrence in practical engineering problems, results presented in this section are restricted to n-hyper-rectangles in $\mathfrak{R}^n$, which, being the Cartesian product of n closed intervals in $\mathfrak{R}$, have 2^n vertices and $2n$ facets.

The *n*-hyper-rectangular required solutions tube S_R is obtained by imposing robustness criteria directly linked to the original mission and system requirements. In particular, R is constrained to be smaller than 10 km, V to be at most 415 m/s and not smaller than the nominal trajectory value minus 30 m/s (in order to reach the transonic regime), the angle of attack and the pitch rate to track the nominal response with a maximum deviation at most of 2.5deg and 5 deg/s, respectively. No requirements are posed on the other variables, even though they are fictitiously constrained by a sufficiently large bound, in order to comply with the required solutions tube definition given here (see assumption 3). From these robustness criteria, it is straightforward to define a *n*-hyper-rectangular, time-varying S_R, taking into account the weight vector and the nominal trajectory.

Table 3 shows the ranges in which the initial state is assumed to be dispersed derived from mission analysis. This determines X_0. The uncertain parameters are assumed to range in the previously defined set Π. Similarly to the previous section's analysis, additional results are shown, obtained with half the initial state dispersion and with the uncertain parameters varying in their 1σ ranges, i.e. $X'_0 = 0.5 \cdot X_0$, $\Pi' = 0.5 \cdot \Pi$. Table 4 shows the results of the application of the proposed technique, as well as the proposed algorithm's execution times on the same PC used for the LTI analysis.

The system is found to be not FTS with respect to $\{[0, T], X_0, S_R(\cdot), \Pi\}$. The first time sample at which an exit from S_R is detected is around 40 s., which is coherent with the local instability found by the LTI analysis. On the other hand, the system is FTS w.r.t. $\{[0, T], X'_0, S_R(\cdot), \Pi'\}$, and an estimate of the robustness margin is $\bar{\gamma} = 3.3 \cdot 10^{-4}$. Fig. 6 compares the $v_0 \cdot v_\pi$ dispersed trajectories used for the FTSV with the required solutions tube for the two cases. Results are projected in the angle of attack, which turned out to be the more critical state variable in terms of FTS. It results that the LTI instabilities ascertained in the previous section do not reflect an actual divergence of the dispersed trajectories, but only cause a violation of tracking requirements under full initial state dispersion and uncertainties, which is recovered in the second case.

This last result shows that the local instability found using the LTI analysis does not compromise the success of the mission; therefore no further effort is required to improve the FCL performance in the X'_0, Π' case. Furthermore, the required computational effort is drastically reduced with respect to LTI-based analyses. These results point out the ability of the proposed approach to overcome the limitations of the current frozen-time practice, by taking into account quantitative dispersions of the system trajectories about the nominal one and evaluating concurrently initial state displacement and uncertain parameters effects. This is done without resorting to computationally intensive techniques, such as Monte Carlo ones, which can thus be ran when the FCL design has already acquired a higher degree of maturity, with a significant gain in the overall efficiency of the FCL design cycle.

Finally, an evaluation is presented of the amount of conservatism introduced by claim 1 in estimating the dispersion of system (1) solutions induced by all the perturbing terms norm-bounded by a value. This is performed with the main intent of showing the potential of the proposed approach in handling problems of practical engineering interest, without pretending to thoroughly characterize the related conservatism. To this end, the present application case is used to compare the $r_1(t_k)$ values obtained by applying the proposed method with a probabilistic estimate of the worst-case infinity vector norm of the solutions of system (9) under a unitary norm-bounded $\boldsymbol{d}(\cdot)$. In order to achieve it, a statistical description of the possible perturbing signals is artificially induced, by assuming $\boldsymbol{d}(\cdot)$ to be piecewise linear in time, and that its values at each time sample t_k are uniformly distributed within the unitary closed ball B_1 and are independent from the values at other time epochs. Then, a well-known randomized algorithm (see Algorithm 2 in [23], for a detailed description) is applied to compute the maximum infinity norm of the resulting dispersion $\boldsymbol{\xi}(t_k)$. In particular, under the assumptions on the perturbing signals' statistical description, using 6905 randomly chosen numerical simulations an estimate $\hat{r}(t_k)$ is obtained such that $\Pr\{|\boldsymbol{\xi}(t_k)|_\infty \leq \hat{r}(t_k)\} \geq 0.999$, with probability 0.999. The capability of capturing the worst-case deviation within these assumptions is questionable, but in the present context it is instrumental in obtaining a meaningful term of comparison for

r_1. More precisely, $\hat{r}(t_k)$ represents a lower bound for the real worst-case dispersion, because the employed randomized algorithm computes $\hat{r}(t_k)$ as the maximum among a finite number of numerical simulations. This in turn implies that the conservatism of the proposed approach will not be worse than the one estimated by such a comparison. Fig. 7 compares the values of r_1 and $\hat{r}$ in all the t_k, pointing out that the conservatism introduced by claim 1 in the considered test cases is significant, but still sufficiently limited as to obtain meaningful indications on which perturbations may be tolerated by the system while remaining FTS.

5 Conclusion

This paper investigates the problem of developing a robustness analysis technique capable of complementing the results of classical LTI based analysis, without requiring a significant computational burden. This is done by exploiting the FTS of LTV systems insisting on a compact time domain and subject to variations in the initial states and to unknown parametric disturbances. A necessary and sufficient condition is provided for the FTS, which requires verifying the FTS property on a limited number of trajectories, based on assuming initial conditions and unknown parameters both vary within polytopes. Based on this result, an approach is proposed to determine also to which extent the LTV system may be perturbed by norm-bounded, time-varying signals, possibly nonlinearly depending on the system state, while remaining FTS. The approach yields a conservative estimate of the maximum norm-bound of the perturbations.

Results of the application of the proposed approach to the augmented longitudinal dynamics of a technology demonstrator of the terminal flight phases of re-entry manoeuvres are shown. Specifically, the approach is applied to the LTV system obtained by linearization of the demonstrator nonlinear dynamics around a time-varying nominal trajectory derived by mission analyses. By comparison with conventional LTI-based analyses, results demonstrate the approach effectiveness in complementing the current frozen-time practice. In addition, the proposed approach is shown to be capable of quantitatively evaluating the dispersion of the system trajectories around the nominal one as a consequence of concurrent initial state

displacement and uncertain parameters effects. These results are achieved without resorting to computationally intensive techniques, such as Monte Carlo ones, which can thus be run when the FCL design has acquired a higher degree of maturity, with an increase in the overall efficiency of the FCL design cycle.

Concerning the computational load, the approach's efficiency depends on some features of the involved polytopes, such as the number of their vertices and facets. Since these numbers may largely vary for general polytopes, it is expected that the approach would be way more effective in dealing with high-dimensional problems by exploiting the peculiarities of a specific class of polytopes. One possibility is to refer to zonotopes, which cover a broad application area (including hyper-rectangles) and are a set of polytopes closed under Minkowski addition and linear transformations, as it is required by the present approach. In addition, zonotope-based methods have the potential to give rise to polynomial total time algorithms, as it is also suggested by the recent literature in the framework of hybrid systems reachability analysis [24]. Further work will be focused on exploiting this possibility.

References

1. **Lu, P.** Regulation about time-varying trajectories: precision entry guidance illustrated. *AIAA J. Guid. Control Dyn*. Vol.22, No.6, pp. 784-790, Nov.-Dec. 1999
2. **Tancredi, U., Grassi, M., Corraro, F., Filippone, E.** Robustness Analysis for Terminal Phases of Re-entry Flight. *AIAA J. Guid. Control Dyn.* Vol. 32, No. 5, September–October 2009.
3. **Cobleigh, B. R**. Development of the X-33 Aerodynamic Uncertainty Model. NASA/TP-1998-206544, 1998.
4. **Leith D. J.,** and **Leithead W. E.** Survey of gain-scheduling analysis and design. *International Journal of Control*, Vol. 73, No. 11, 2000, pp. 1001-1025.
5. **Fujimori, A., Nikiforuk, P.N.**, and **Gupta, M.M.** A Flight Control Design of a Re-Entry Vehicle Using a Double-Loop Control System with Fuzzy Gain Scheduling. *Proceedings of the Institution of Mechanical Engineers*, Vol. 215, Part G, pp. 1-12. 2001

6. **Bayle, G. P.** Space Shuttle entry flight control off-nominal design considerations. *AIAA J. Guid. Control Dyn.*, Vol. 7, No.1, 1984, pp. 9-14-
7. **Shwani, C., Nguyen, V., Tran, H., Poladian, D., Falangas, E.** Dynamics and Stability and Control Characteristics of the X-37. In Proceedings of the AIAA Guidance and Control Conference, Montreal, Canada, 2001, AIAA paper 2001-4383.
8. **Korte, U.** Tasks and Needs of the Industrial Clearance Process. In *Advanced Techniques for Clearance of Flight Control Laws*, Springer-Verlag, Berlin, 2002, pp. 13-33.
9. **Gayek, J.E.** A survey of techniques for approximating reachable and controllable sets. Proceedings of the 30th Conference on Decision and Control Brighton, UK, pages 1724–1730, 1991.
10. **Girard**, **A.** Reachability of uncertain linear systems using zonotopes. In *Hybrid Systems: Computation and Control*, Lecture Notes in Computer Science Series, Vol. 3414, Springer, New York, 2005, pp 291-305.
11. **Dorato, P.** An Overview of Finite-Time Stability.In *Current Trends in Nonlinear Systems and Control*, Systems and Control: Foundations & Applications, 2006, Part II, 185-194.
12. **Grujic, L. T., Richard, J. P., Borne, P.,** and **Gentina, J. C**. *Stability Domains.* Chapman & Hall/CRC, Boca Raton, FL, 2000, ch. 6.
13. **Amato, F., Ariola, M.,** and **Dorato, P.** Finite time control of linear systems subject to parametric uncertainties and disturbances. *Automatica*, Vol.37, No.9, pp. 1459-1463, Sept. 2001.
14. **Jönsson, U.** Robustness of trajectories with finite time extent. *Automatica*, Vol. 38, No.9, pp.1485-1497, 2002.
15. **Graettinger, T. J.,** and **Krogh, B. H**. Hyperplane method for reachable state estimation for linear time-invariant systems. *Journal of Optimization Theory and Applications*, Vol. 69, No. 3, 1991, pp. 555-588.
16. **Ziegler, G. M.** *Lectures on Polytopes*, Graduate Texts in Mathematics 152, Springer-Verlag, New York, 1995.
17. **Fukuda, K.** and **Weibel, C.** Computing all faces of the Minkowski sum of V-polytopes. In Proc. 17th Canadian Conf. Computational Geometry, 2005, pp. 253-256.
18. **Ottmann, T., Schuierer, S.,** and **Soundaralakshmi, S.** Enumerating extreme points in higher dimensions. *Nordic J. Computing*, Vol. 8, No. 2, pp. 179 – 192, 2001.

19. **Corraro, F., Filippone, E., Russo, M., Verde, L., Tancredi, U., Moccia, A.,** and **Grassi, M.** Flight dynamic characterisation of the USV-flying test bed vehicle. In Proceedings of AIAA/CIRA 13th Int. Space Planes and Hypersonic Syst. and Technologies Conf., AIAA-2005-3276, Capua, Italy, 2005.
20. **Etkin, B.,** and **Reid, L.D**., *Dynamics of Flight: Stability and Control*, 3rd ed., John Wiley and Sons, Inc, New York, 1996.
21. **Rufolo, G., Roncioni, P., Marini, M., Votta, R.,** and **Palazzo, S.** Experimental and Numerical aerodynamic data integration and aerodatabase development for the PRORA-USV-FTB_1 reusable vehicle. In Proceedings of the AIAA/AHI 14th Int. Space Planes and Hypersonic Syst. and Technologies Conf., AIAA-2006-8031, Canberra, Australia, 2006.
22. **Tancredi, U., Grassi, M., Corraro, F., Filippone, E.,** and **M. Russo**. A Novel Approach to Clearance of Flight Control Laws over Time Varying Trajectories. *Automatic control in aerospace*, ISSN 1974-5168, Vol.1, n.1, 2008.
23. **Calafiore, G., Dabbene, F.,** and **Tempo, R.** A survey of randomized algorithms for control synthesis and performance verification. *J. Complexity*, Vol.23, No. 3, pp. 301-316, Jun. 2007.
24. **Girard, A.** Reachability of uncertain linear systems using zonotopes. In *Hybrid Systems: Computation and Control*, (Lecture Notes in Computer Science Series, Vol. 3414), Springer, New York, 2005, pp 291-305.

Appendix: Notation

b	Uncertainties space dimension
B_r	Closed ball in $\Re^n$ of radius r
c	Mean aerodynamic chord
C^0	Set of all continuous bounded real matrix functions on an interval
C_L	Lift coefficient
C_D	Drag coefficient
C_m	Pitching moment coefficient
$\boldsymbol{d}$	Perturbing term

$\boldsymbol{e}_i$	i-th versor of the standard basis of $\mathfrak{R}^n$
g	Gravity acceleration
h	Altitude
k_i	Control gains
$\mathbf{I}$	Identity matrix
I_{yy}	Moment of inertia about the pitch axis
m	Number of facets of the required solutions tube
m_v	Mass of the vehicle
M	Mach number
n	State space dimension
q	Pitch rate
q_∞	Dynamic pressure
R	Range
s	Scaling function
S	Solutions tube
S_R	Required solutions tube
t	Time
T	Time domain length
V	Air relative velocity
α	Angle of attack
γ	Robustness margin
δ_e	Elevons symmetric deflection
ζ	Feedback state
θ	Pitch angle

$\boldsymbol{\pi}$ Uncertain parameters vector

$\boldsymbol{\Phi}$ Transition matrix

σ Standard deviation

Σ Aerodynamic reference surface

Subscripts and Superscripts

$( )_{D0}$ Variable relative to bias uncertainties on C_D

$( )_{D\alpha}$ Variable relative to uncertainties of α on C_D

$( )_{d}$ Variable relative to the perturbed system

$( )_{L0}$ Variable relative to bias uncertainties on C_L

$( )_{m0}$ Variable relative to bias uncertainties on C_m

$( )_{m\alpha}$ Variable relative to uncertainties of α on C_m

$( )_{m\delta}$ Variable relative to uncertainties of δ_e on C_m

$( )^{Tr}$ True value

$( )^{(i)}$ Variable relative to the i-th vertex of a polytope

$\langle \cdot,\cdot \rangle$ Standard inner product in $\mathfrak{R}^n$

$| \cdot |$ Absolute value of a real number

$| \cdot |_p$ Vector and induced matrix p-norm

$\| \cdot \|_\infty$ L_∞ norm

$\mathfrak{R}$ Set of real numbers

$\mathfrak{R}_+$ Set of positive real numbers

Illustrations of the paper: A linear time varying approach for robustness analyses of a re-entry flight technology demonstrator

Fig. 1 FTB1 vehicle

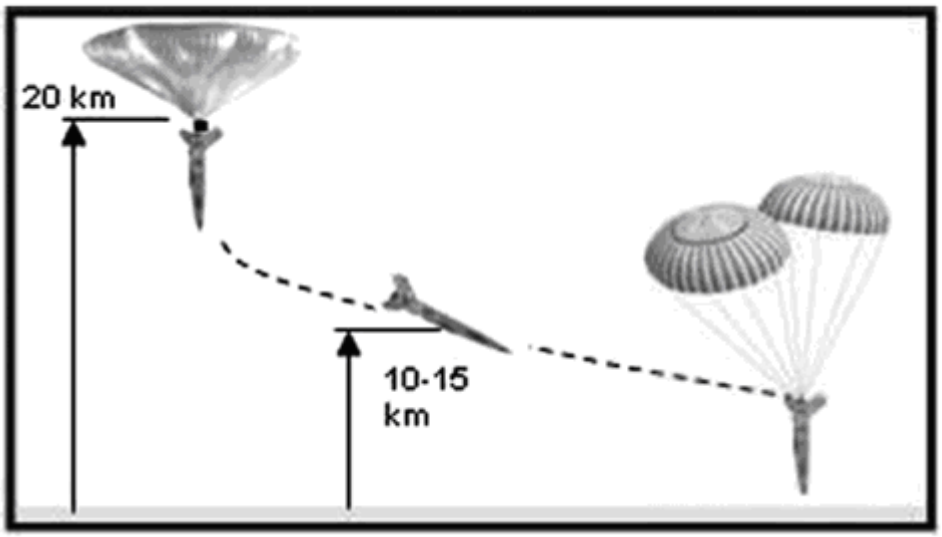

Fig. 2 Nominal profile of the first FTB1 mission

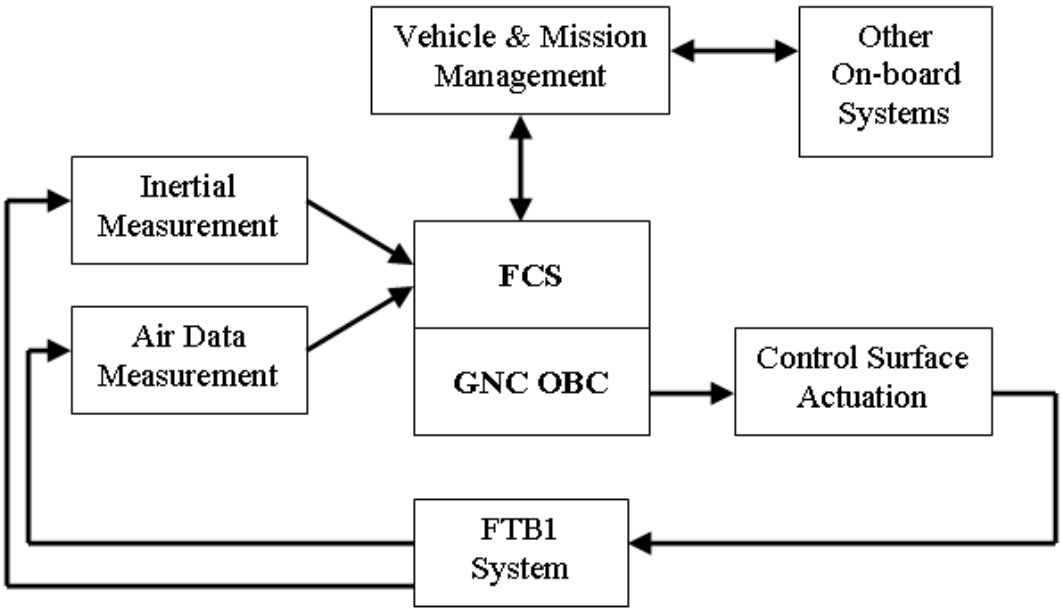

Fig. 3 FCS functional architecture

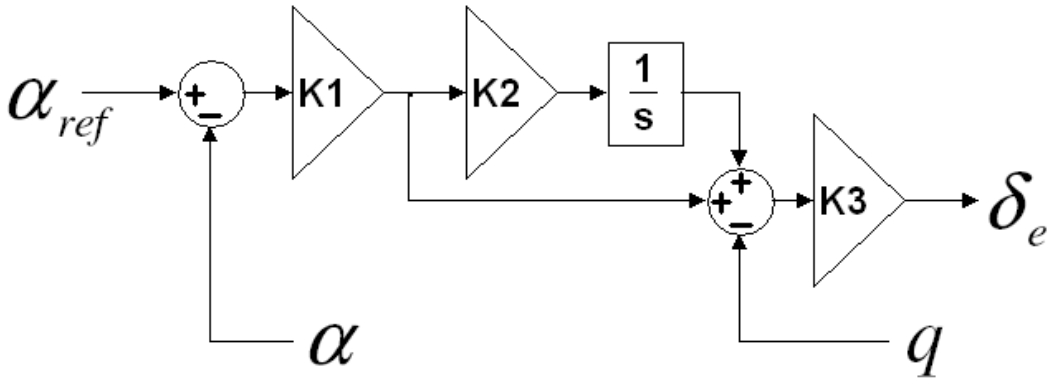

Fig. 4 Longitudinal flight control law

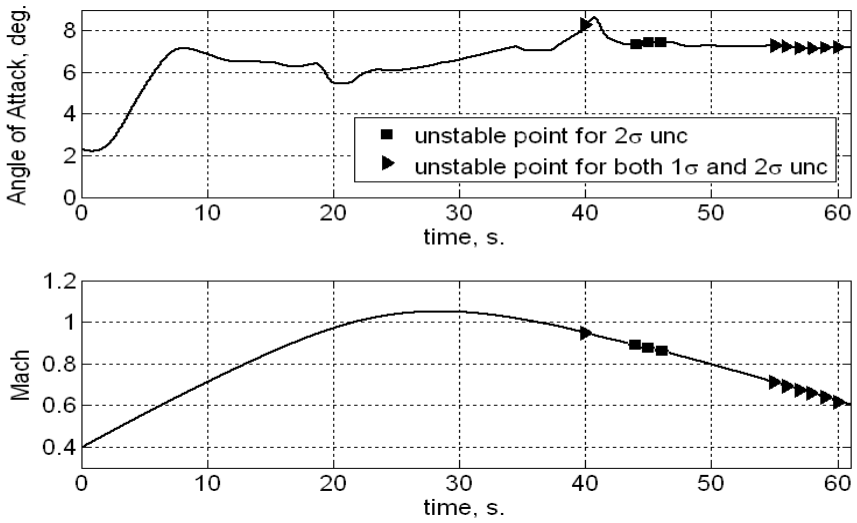

Fig. 5 FTB1 nominal trajectory with marked unstable epochs

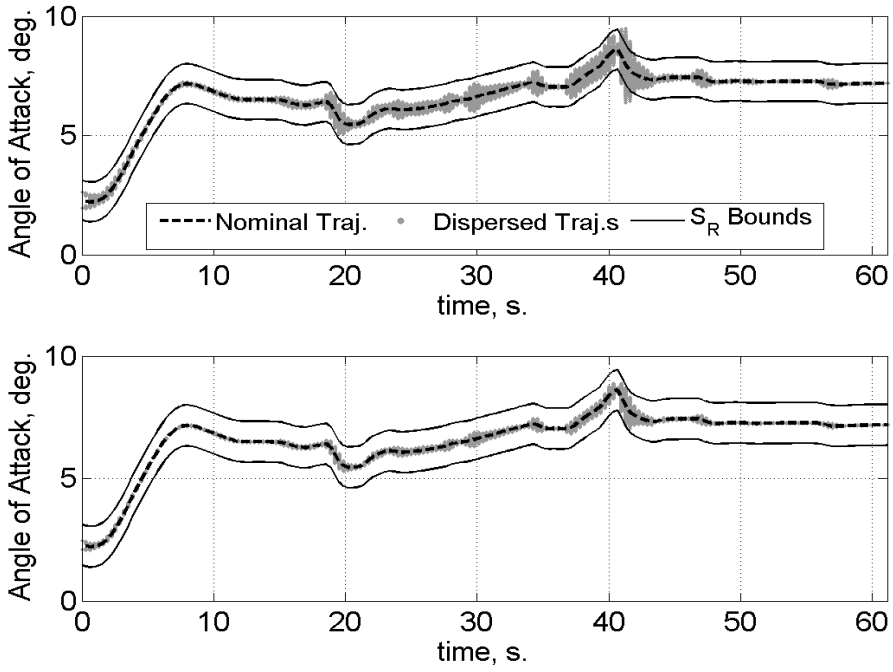

Fig. 6 Angle of attack trajectories dispersion under X_0, Π (top) and X'_0, Π' (bottom).

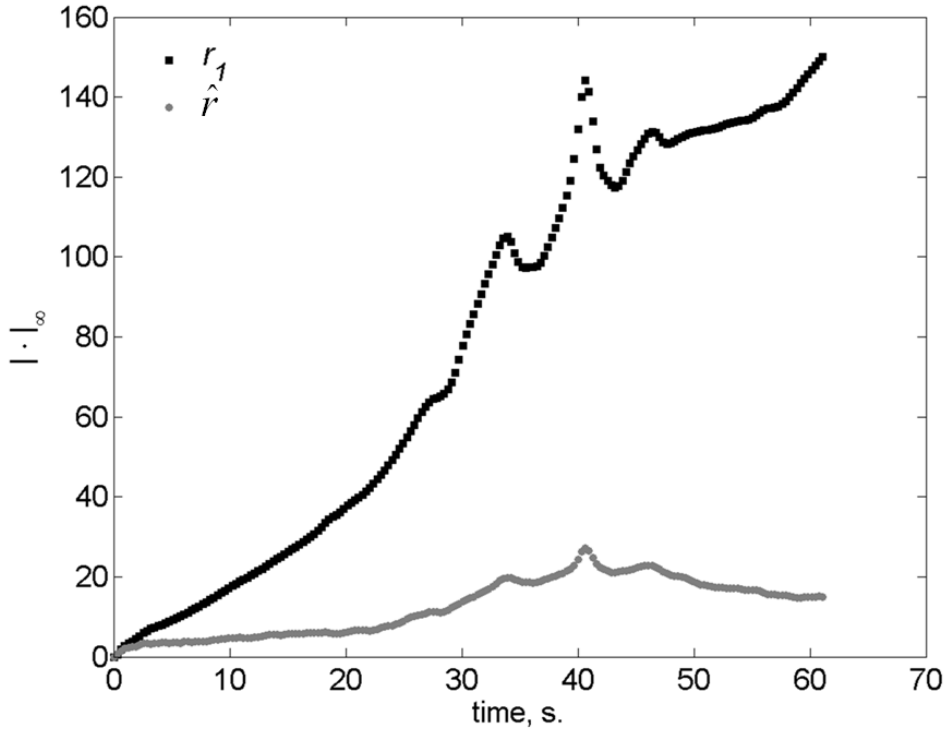

Fig. 7 Worst-case dispersions under a unitary norm-bounded $\boldsymbol{d}(\cdot)$: r_1 (black) vs. $\hat{r}$ (gray)

Tables of the paper: A linear time varying approach for robustness analyses of a re-entry flight technology demonstrator

Table 1 Mission and GNC requirements for FTB1 first mission

Release Altitude	20 Km
Maximum Mach Number	1.05
Experimental Requirements	Constant Angle of Attack in Transonic Regime of Flight Target Transonic Angle of Attack = 7 deg Load Factor Along Vehicle Z-Body Axis ≤ 3g Load Factor Along Vehicle X-Body Axis ≤ 1.5g
GNC Requirements	Longitudinal Flight with Angle of Attack Tracking Tracking Error ≤ ± 1 deg (RMS) ± 2.5 deg (Max)
Parachute Deployment	Between Mach 1.2 and 0.6

Table 2 LTI Stability Analysis Results

Uncertainty Space	Is locally Stable?	Unstable Epochs (s)	Max. Eigenvalue Real Part
Π	No	$T_{40} = 40.00$	0.0308
		$T_{44} = 44.00$	0.0089
		$T_{45} = 45.00$	0.0077
		$T_{46} = 46.00$	0.0070
		$T_{56} = 56.00$	0.0020
		$T_{57} = 57.00$	0.0024
		$T_{58} = 58.00$	0.0027
		$T_{59} = 59.00$	0.0028
		$T_{60} = 60.00$	0.0030
		$T_{61} = 61.00$	0.0031
Π'	No	$T_{40} = 40.00$	0.0230
		$T_{56} = 56.00$	0.0018
		$T_{57} = 57.00$	0.0022
		$T_{58} = 58.00$	0.0025
		$T_{59} = 59.00$	0.0027
		$T_{60} = 60.00$	0.0028
		$T_{61} = 61.00$	0.0029

Table 3 Initial State Dispersion Ranges

	V	α	q	h	R	Θ	ζ

Variable	m/s	deg	deg/s	m	M	deg	deg/s
Min	-10	-1	-0.5	-500	-2	-1.5	-0.1
Max	10	1	0.5	500	2	2	0.5

Table 4 LTV Analysis Results

Input sets used	FTSV solution			RMD solution	
	Is FTS?	Exit t s	CPU t s	$\bar{\gamma}$	CPU t s
X_0, Π	No	40.64	4.3	N.A.*	N.A.*
X'_0, Π'	Yes	N.A.*	4.3	$3.3 \cdot 10^{-4}$	2.1

* N.A. = Not Available